A Manipulation Framework for Compliant Humanoid COMAN: Application to a Valve Turning Task

Arash Ajoudani, Jinoh Lee, Alessio Rocchi, Mirko Ferrati, Enrico Mingo Hoffman, Alessandro Settimi, Darwin. G. Caldwell, Antonio Bicchi, and Nikos G. Tsagarakis

***Abstract*— With the purpose of achieving a desired interaction performance for our compliant humanoid robot (COMAN), in this paper we propose a semi-autonomous control framework and evaluate it experimentally in a valve turning setup. The control structure consists of various modules and interfaces to identify the valve, locate the robot in front of it and perform the manipulation. The manipulation module implements four motion primitives (Reach, Grasp, Rotate and Disengage) and realizes the corresponding desired impedance profile for each phase to accomplish the task. In this direction, to establish a stable and compliant contact between the valve and the robot hands, while being able to generate the sufficient rotational torques depending on the valve's friction, Rotate incorporates a novel dual-arm impedance control technique to plan and realize a task-appropriate impedance profile. Results of the implementation of the proposed control framework are firstly evaluated in simulation studies using Gazebo. Subsequent experimental results highlight the efficiency of the proposed impedance planning and control in generation of the required interaction forces to accomplish the task.**

I. INTRODUCTION

Over the years, the occurrence of major adverse events resulting from the natural processes of the Earth (e.g. earthquakes, floods, etc), their consequences (e.g. Fukushima disaster), and system faults and failures (e.g. Chernobyl disaster) have caused countless deaths and property damage. Due to the inevitable nature of such catastrophes, it is extremely important to employ effective and efficient robotic systems to assist in the execution of the tasks in unstructured and hostile environments. This will, however, cause intense human-robot interaction challenges for the victims and the operators, highlighting the need for the humanoid robots to robustly and safely interact with uncertain environments [1].

Some of the requirements have been addressed by introducing variable stiffness or torque controlled robots which can tune the physical characteristics of their joints by active or passive control techniques [2]–[4]. Other avenues of research seek for the creation of robust control frameworks for such systems with high degrees of freedom (DOF) [5]–[7] to provide capabilities to adapt to features of the environment.

With the aim to realize a robust manipulation framework, in this work, a realtime control architecture for our intrinsically compliant humanoid robot (COMAN [2]) is developed and its functionality and performance is verified by preliminary experimental trials. The proposed control framework incorporates various modules with an interface between the higher-level sensing and the lower-level control. While our final goal is to realize a fully autonomous system, currently, the user intention is combined with the autonomy of the robot controller to perform a valve turning task, a realistic example of prevention or disaster response, which has been chosen as one of the target tasks for the DARPA Robotics Challenge (DRC) [8].

The problem of robotic valve turning has been investigated in some studies: in [9], an arm-aircraft system for valve turning is presented and experimentally validated. In this work, a teleoperation interface is developed to actuate the manipulators and perform the turning operation. Authors in [10] propose a whole-body control architecture for a humanoid robot to perform heavy tasks such as pushing a wall and twisting a valve. In another setup, a kuka lightweight robot arm is utilized to manipulate the valve using an imitation learning approach [11]. An extended Kalman filter is adopted to improve the accuracy of the sensed valve position and a decision rule is implemented using a fuzzy system.

It is well-known that to achieve an effective interaction with the uncertain environment, task-efficient restoring forces must be applied in response to the environmental displacements. To establish such a relation, Cartesian impedance control, as a well recognized framework can be utilized to realize a desired and task-efficient [12] Cartesian stiffness matrix. As a result, a target manipulation task can be executed effectively and naturally. To that end, this paper pretenses an alternative solution to the robotic valve turning problem, benefiting from the physical compliance and active control techniques. In this direction, a novel dual-arm impedance control framework is developed and integrated into the control architecture of our intrinsically compliant robot. The proposed interaction controller avoids the generation of high interaction forces along the constraint directions of the hands in contact with the valve. In the meantime, task-efficient rotational torques are applied to turn the valve. This is achieved due to the implementation of an update law in our manipulation framework to adjust the realized Cartesian stiffness profile of the arms depending on the existing valve joint friction.

The rest of the paper is structured as follows: our intrinsically compliant humanoid robot and the software interfaces are introduced in section II. The control architecture, mainly

Authors are with the Dept. of Advanced Robotics, Istituto Italiano di Tecnologia, Via Morego 30, 16163, Genova, Italy. Arash Ajoudani, Mirko Ferrati and Antonio Bicchi are also with Interdepartmental Research Centre "E. Piaggio", Faculty of Engineering, University of Pisa (e-mails: {Arash.Ajoudani, Jinoh.Lee, Alessio.Rocchi, Enrico.Mingo, Alessandro.Settimi, Nikos.Tsagarakis, Darwin.Caldwell}@iit.it, mirko.ferrati@gmail.com and bicchi@centropiaggio.unipi.it).

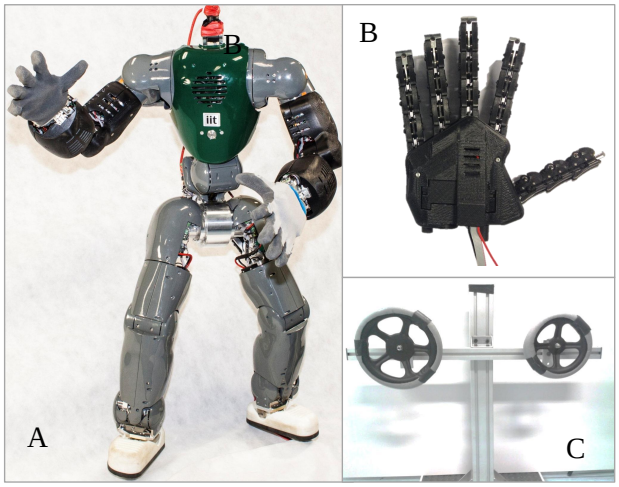

Fig. 1: COMAN robot (A), Pisa/IIT SoftHand (B) and the adjustable friction valve setup (C).

focusing on the manipulation framework, is discussed in section III. Results of the implementation of the proposed control framework in simulation studies and real experiments are reported in section IV. Finally, section V addresses the conclusions.

II. Intrinsically Compliant Humanoid

A. COMAN

COMAN [2] (Fig. 1. A) is a torque controlled robot with 31-DOF, 14 of which are based on Series Elastic Actuation that is used to enhance the physical interaction performance of the robot. The robot has 6 DOFs for each leg, 7 DOFs in each arm, 3 DOFs in the waist, 2 DOFs in the neck, and is equipped with two Pisa/IIT SoftHands (see next section). The passive compliance of the joints are effective to absorb the high bandwidth impacts. Each joint provides position, velocity and torque sensing, while decentralized position and active impedance control are built in each DSP board at 1KHz RT. The robot is equipped with an IMU in the waist and four 6-axes force/torque sensors in the ankles and the forearms. The robot will have a Carnegie Robotics MultiSense S7 sensor[1] mounted as a head, but we are currently using an RGB-D camera (Asus Xtion Pro Live) mounted above the torso and two cameras strapped at the forearms for perception.

B. Pisa/IIT SoftHand

To solve for the control complexity problem and the robustness issues raised by the usage of the poly-articulated hands, the Pisa/IIT SoftHand (Fig. 1. B, [13]) was developed in a partnership between the "E. Piaggio" center of the University of Pisa and the Advanced Robotics department of the Italian Institute of Technology. Using the adaptive synergy concept [14], the anthropomorphic hand was designed with 19 DOFs and actuated by one DC motor which drives the hand joints along the first synergy of the human hand movement. To address the robustness issues, SoftHand incorporates rolling contact joints with elastic ligaments which ensure anatomically correct motion when actuated, but easily disengage on impact to allow safe interaction with the uncertain environment. The elastic ligaments also allow deformation while ensuring the hand returns to its original configuration.

C. Robot Interfaces

The robot is controlled using the YARP [15] framework while all the perception is handled by the ROS framework [16]. The low-level library *Robolli* communicates with the DSP boards, while YARP is used for high-level communication between control modules. The DSP boards implement a decentralized joint impedance control running at 1kHz real-time. The *comanInterface* module uses the *Robolli* library to expose the DSP functionalities at the YARP level, where we have access to impedance control, joint configuration, speed and torque measurements, IMU readings and force-torque readings at the ankles and forearms, again at 1kHz. The manipulation (*valveTurnModule*) module is written using YARP functionalities while the kinematic and dynamic model of the robot is specified using the URDF[2] format, parsed by the IdynTree[3] library to obtain forward kinematics, Jacobians and dynamics data. This module complies to a simple communication protocol to control state transitions in an internal state machine. In particular *start* and *stop* commands can be issued on a *switch* input port, while by writing Cartesian coordinates on the *valve−data* input port an external sensing module can provide the manipulation module a relative position/orientation of the valve w.r.t. the torso frame of reference, Σ_t. Lastly, a *command:i* port accepts manipulation primitives to reach to the object, grasp it, manipulate it (rotate the valve), release it, and disengage (the overall system infrastructure is depicted in Fig. 2).

The valve is reached by the robot through a walking (*flatWalk*) module that accepts forward, lateral, and rotate in place commands. The *Pilot Interface* [17] shows the actual configuration of the robot and the point cloud of the scene given by a 3D camera which is used to recognize the valve with respect to a robot local frame of reference (see Fig. 3).

III. Control Architecture

A. Motion Primitives

As mentioned above, the valve data (position and the orientation of the center of rotation, and the valve radius) is sensed using an RGB-D camera and translated and defined in the torso frame of reference, Σ_t, to take into account the required adjustments due to the lower-body movements. The manipulation module first calculates two sets of desired grasping position and orientation for the right and left hand, with a small offset distance from the valve chassis. Consequently,

[1] http://carnegierobotics.com/multisense-s7/

[2] http://wiki.ros.org/urdf

[3] http://wiki.icub.org/codyco/dox/html/group-iDynTree.html

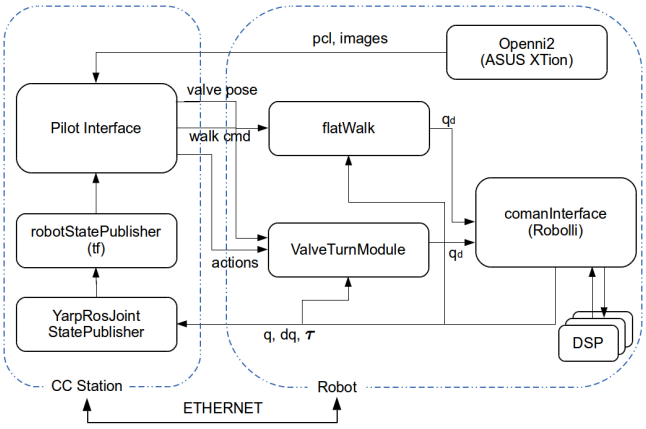

Fig. 2: System Architecture of the *valve experiment*.

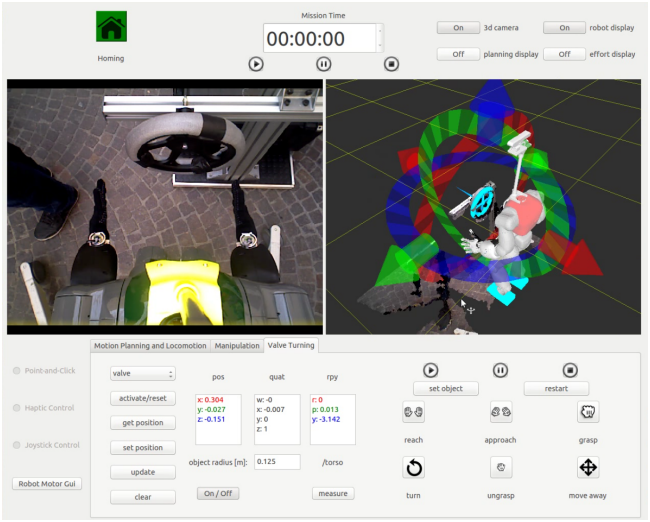

Fig. 3: The 3D valve model is overimposed on the 3D scene, and commands are sent by a dedicated GUI.

the valve turning task is broken down into four motion primitives: reaching (Reach), approaching to[4]/grasping the valve (Grasp), rotating the valve (Rotate) and releasing/moving far from the valve (Disengage). The transition between the phases of the task is achieved using a state machine paradigm and can be controlled/interfered by the user. With the aim to maintain the body balance, COMAN lower-body is controlled by a stabilization framework, previously proposed in [18]. However, in presence of higher external forces in more intensive manipulation tasks (such as debris removal), this problem must be addressed in a whole-body framework [5].

Reaching primitive utilizes the right, ${}^{T}_{e}\mathbf{J}_R(q)$, and the left, ${}^{T}_{e}\mathbf{J}_L(q)$, arm end-effector Jacobians (with respect to the torso frame of reference, see Fig. 4) and implements a closed loop inverse kinematics algorithm (CLIK) to reach

[4]Approach motion primitive finely adjusts positions of the two hands to facilitate the grasping of the valve frame.

[5]For instance by including the center of mass Jacobian in the control architecture [19].

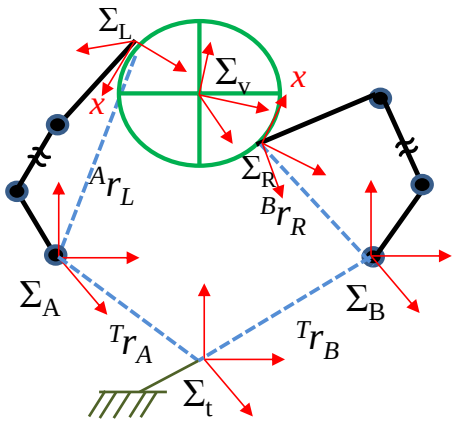

Fig. 4: Dual-arm valve turning setup. The grasping locations are planned by the manipulation module in such a way that the left and the right arm end-effectors along x direction are always tangent to the valve curvature, enabling the torque generation around its axis of rotation. This consideration facilitates the trajectory generation and impedance planning in rotation primitive.

to the desired left and right hand positions. Smooth point-to-point trajectories for both hands are generated by the trajectory generation module using a fifth order nonlinear function. Once the SoftHands reach to the desired positions, Grasp primitive makes them approach to the valve and grasp it firmly. Consequently, the circular trajectories (using the developed trajectory generation module) are built for both hands, by taking into account the valve data, and realized by the impedance controllers of the arms (see section below). The rotation angle can be re-defined using the pilot interface. A singularity robust generalized inverse [20] is implemented for all phases while the self motion of the two arms are controlled by projecting the gradient of a cost function proposed in [21] into the nullspace of the arm Jacobians to possibly avoid the occurrence of the joint limits.

B. Interaction Control

To render a desired interaction performance using our manipulation control framework, the desired Cartesian stiffness matrix is defined in task coordinates and the required joint stiffness values are calculated using the corresponding conservative congruence transformation [22]. Even though the realization of the desired Cartesian stiffness matrix will be subject to uncertainty due to the inadequacy[6] of the control parameters in joint coordinates (i.e. joint stiffness), the implementation of the joint impedance controller is preferred over the pure torque control technique due to its improved robustness and stability [25].

To plan for the variable impedance, during the Reaching and Disengage phases, a relatively compliant and fixed Cartesian stiffness matrix, ${}^{T}\mathbf{K}_d \in \mathbb{R}^{6\times6}$, is defined at left arm end-effector (Σ_L) and right arm end-effector (Σ_R) frames with respect to Σ_t. This consideration is taken into account to

[6]Two possible directions can be pursued to issue this problem: integration of the configuration dependent stiffness control [23], or using a torque control approach [24].

avoid the generation of high interaction forces in case of any unexpected collision with the environment. Consequently, the required joint stiffness values of each arm ($\mathbf{K}_{J_R}$ and $\mathbf{K}_{J_L}$) are calculated using the following linear optimization problem

$$\begin{aligned} &\text{minimize} \quad \|\mathbf{K}_J \; - \; {}^{T}_{e}\mathbf{J}(q)^T \; {}^{T}\mathbf{K}_d \; {}^{T}_{e}\mathbf{J}(q)\| \\ &\text{subject to} \quad k_{J_{i-min}} < k_{J_i} < k_{J_{i-max}} \end{aligned} \tag{1}$$

with ${}^{T}_{e}\mathbf{J}(q)$ and $\mathbf{K}_J$ being the Jacobian and the diagonal joint stiffness matrices of the corresponding arm. The above optimization is performed for both arms separately and synchronously. $\|.\|$ symbolizes the Frobenius norm operator, and $k_{J_{i-min}}$ and $k_{J_{i-max}}$ correspond the minimum and maximum allowable (which take into account the stability boundaries for COMAN's joint impedance controller [25]) joint stiffness gain of the ith arm joint, where $i \in \mathbb{R}^7$.

While rotating, the aim is to realize a robust and stable contact between the valve and the two arm end-effectors. Therefore, it is essential to avoid the generation of high interaction forces between the two hands and the valve frame. To achieve this, we consider a diagonal desired stiffness matrix ${}^{e}\mathbf{K}_{c_d} \in R^{6\times 6}$, with respect to the end-effector frames as follows

$${}^{e}\mathbf{K}_{c_d} = \begin{bmatrix} k_{x_d} & k_{y_d} & k_{z_d} & k_{\alpha_d} & k_{\beta_d} & k_{\gamma_d} \end{bmatrix}_{\text{diag}}, \tag{2}$$

with $[k_{x_d} \; k_{y_d} \; k_{z_d}]$ and $[k_{\alpha_d} \; k_{\beta_d} \; k_{\gamma_d}]$ corresponding to translational and rotational components of the desired stiffness matrix, respectively. These components are chosen experimentally, to render a compliant stiffness profile at the arm end-effectors.

To establish the transformation between the desired Cartesian stiffness matrix with respect to the end-effector frames Σ_L and Σ_R, and the corresponding arm joint stiffness values, we can write

$$\hat{\mathbf{R}} = \begin{bmatrix} {}^{e}_{T}\mathbf{R} & \mathbf{0}_{3\times 3} \\ \mathbf{0}_{3\times 3} & {}^{e}_{T}\mathbf{R} \end{bmatrix}, \tag{3}$$

$${}^{e}_{e}\mathbf{J}(q) = \hat{\mathbf{R}} \; {}^{T}_{e}\mathbf{J}(q), \tag{4}$$

with ${}^{e}_{T}\mathbf{R} = {}^{T}_{e}\mathbf{R}^T$, denoting the rotational matrix of the torso with respect to the corresponding end-effector frame. Now, we can identify the required joint stiffness values of the both arms using the following optimization target

$$\begin{aligned} &\text{minimize} \quad \|\mathbf{K}_J \; - \; {}^{e}_{e}\mathbf{J}(q)^T \; {}^{e}\mathbf{K}_{c_d} \; {}^{e}_{e}\mathbf{J}(q)\| \\ &\text{subject to} \quad k_{J_{i-min}} < k_{J_i} < k_{J_{i-max}}. \end{aligned} \tag{5}$$

In the meantime, to be able to rotate the valve around its rotation axis (which is defined to coincide with the x direction at the end-effector frames: Σ_L and Σ_R), the Cartesian stiffness component along x direction must be stiff enough to overcome the existing friction of the valve. Here, an update law is implemented to increase the corresponding stiffness parameter, k_{x_d}, to a value that can generate sufficient rotational torques at both arm end-effectors. In this direction, to realize equivalent stiffness profiles for both arms, the Cartesian position error along x direction, e_x, is calculated for both arms and the maximum error value is used to update the stiffness component

$$\begin{aligned} &\text{define} \quad e_x = \max(|x_{d_L} - x_{m_L}|, |x_{d_R} - x_{m_R}|) \\ &\text{if} \quad e_x > \varepsilon_x \\ &\text{update} \quad k_{x_{d_{k+1}}} = k_{x_{d_k}} + c_x \, e_x \end{aligned} \tag{6}$$

with x_{d_L}, x_{m_L}, x_{d_R} and x_{m_L} denoting the desired and measured Cartesian position of the left and the right arm along x direction, respectively. c_x is the update gain, to be identified experimentally; $k_{x_{d_k}}$ and $k_{x_{d_{k+1}}}$ correspond to the old and the updated value of the stiffness component at each iteration. This must be noted here that c_x must be chosen by taking into account the stability of the closed loop system. In addition, this parameter may need to be adjusted if the task requirements meet substantial changes. In our future work we focus on this issue and provide on-line identification of this parameter using interaction torque observers or learning approaches.

To avoid the integration of the stiffness component for small values of e_x, the update law is applied if the position error exceeds a predefined value, ε_x. In addition, to avoid the winding up effect, a saturation level is considered for k_{x_d}, meaning that the update law will be issued until $k_{x_d} < k_{x_{dmax}}$. At each iteration, the required joint stiffness values for both arms are calculated from (5), accordingly.

In all phases, the desired Cartesian damping matrix is designed using a technique proposed in [26], where the desired Cartesian stiffness matrix $\mathbf{K}_d$, is factorized[7] using a nonsingular matrix $\mathbf{Q}$ and a diagonal matrix $\mathbf{B}$ as follows

$$\mathbf{K}_d = \mathbf{Q}\,\mathbf{B}\,\mathbf{Q}^T. \tag{7}$$

Consequently, a diagonal damping matrix $\mathbf{D}_\xi = \text{diag}\{\xi_i\}$ with $\xi_i = 0.7$ denoting the damping coefficient, is formed and used for the planning of the desired Cartesian damping matrix $\mathbf{D}_d$,

$$\mathbf{D}_d = 2\mathbf{Q}\mathbf{D}_\xi \; \mathbf{B}^{\frac{1}{2}} \; \mathbf{Q}^T, \tag{8}$$

and projected into the joint space using the corresponding conservative congruence transformation (see details in [26], [27]). Eventually, calculated joint damping and stiffness parameters are tracked by COMAN's joint impedance controller.

IV. Results

Simulation Environment: Prior to the experiments, the efficiency of the integrated control architecture in rendering a desired motion and interaction performance is evaluated using Gazebo simulator [8]. Gazebo is a well-recognized and open-source simulator that can handle different Dynamic Engines (DART, Bullet, SimBody, and ODE which is used in our simulations). To establish the connection between the COMAN model, our modules and Gazebo, a set of plugins for the Gazebo simulator that enables the interoperability between a robot, controlled using the YARP framework, and Gazebo itself has been implemented [28]. A model of the

[7]Required matrix calculations in C++ environment is implemented using Armadillo library, http://arma.sourceforge.net/.

[8]http://gazebosim.org/

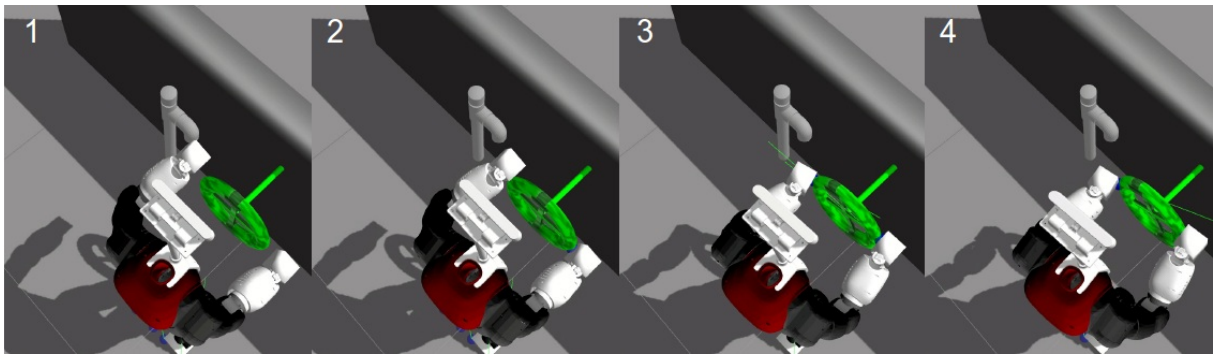

Fig. 5: Simulation results of the valve turning experiment using Gazebo simulator. (1) Dual arm reaching and (2) grasping (pushing towards the valve) motion primitives are followed by (3) rotating and (4) disengage.

valve with friction around the rotation axis is taken from the existing VRC model repository and used in our experiments. Since the SoftHand Gazebo model is still being developed, we use a high friction coefficient between the arm end-effectors and the valve to be able to manipulate it without grasping.

Fig. 5 demonstrates the snapshots of the valve turning experiment in simulations. The most left figure (5.1), illustrates the reaching phase of the arm end-effectors to the desired positions around the valve, calculated by the manipulation module depending on the valve data and the rotation angle. The end-effectors are then pushed towards the valve center of rotation (5.2) to realize a desired friction between the valve and the end-effectors. Consequently, the valve is rotated (5.3) for the predefined rotation angle of the valve and released (5.4). As noted above, simulations are performed to primarily investigate the accuracy of the robot kinematic and dynamic models, as well as the capabilities of the proposed manipulation framework [9].

Experimental Results: Two valves with adjustable values of the torsional springs were mounted on a variable height stand (Fig. 1. C). Using the pilot interface, the COMAN robot was located in front of the valves exploiting flatwalk. Consequently, the valve data was sensed by perception module and used for the planning and control of the desired grasping locations, motion primitives and the impedance profiles using manipulation module.

Figure. 6 illustrates different phases of the task execution where a relatively low and fixed endpoint stiffness profile (with respect to Σ_t, with 200 $\frac{N}{m}$ for translational and 50 $\frac{Nm}{rad}$ for rotational components) was considered for both arm end-effectors during Reaching and Disengage phases. After Reaching, SoftHands grasped the valve and molded around its chassis due to the implemented concept of soft synergies and the existence of passive elasticity in the finger joints. Once the valve was firmly grasped by the two SoftHands, the user triggered the rotation state. In this phase, the desired diagonal Cartesian stiffness matrix (with respect to Σ_L and Σ_R, with $[200\ 100\ 100\ ]\frac{N}{m}$ for translational and 50 $\frac{Nm}{rad}$ for rotational components) was chosen to realize a stable grasp, avoiding the generation of high interaction forces across the two SoftHands ($\approx y$ direction) or perpendicular to the valve surface ($\approx z$ direction).

[9]Details of the simulation environment and some results are illustrated in [17]. In this paper, we aim at evaluating the achieved experimental results.

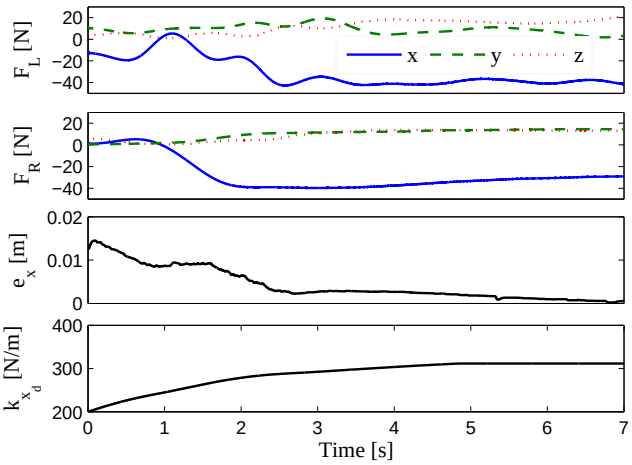

Fig. 7: Two top plots illustrate the acquired interaction forces at the wrist of the SoftHand for left F_L, and the right hand F_R, in rotation phase. The maximum tracking error (e_x) and the updated stiffness parameter (k_{x_d}) are shown in the two bottom plots, respectively.

To overcome the existing friction in the valve axis, the preset Cartesian stiffness component along the valve rotation (x direction in Σ_L and Σ_R) must be updated to comply with the circular motion of the SoftHands around the valve axis. To achieve this, using (5) and (6), the desired stiffness component k_{x_d} was updated and the required joint stiffness values were calculated. Fig. 7 illustrates the interaction forces at the wrist of the SoftHand for the left F_L, and the right arm F_R, in rotation phase. The plots are illustrated from the moment that Rotate motion primitive is executed, which explains why some plots start from non zero values. The maximum tracking error (e_x) and the updated stiffness parameter (k_{x_d}) are shown in the two bottom plots, respectively. As illustrated in these plots, k_{x_d} is efficiently adjusted to overcome the valve joint friction and rotate it. For instance, at the very beginning of this experiment, the error value increases due to the high value of valve friction, until k_{x_d} is adjusted to reduce this error. Subsequently, a very good

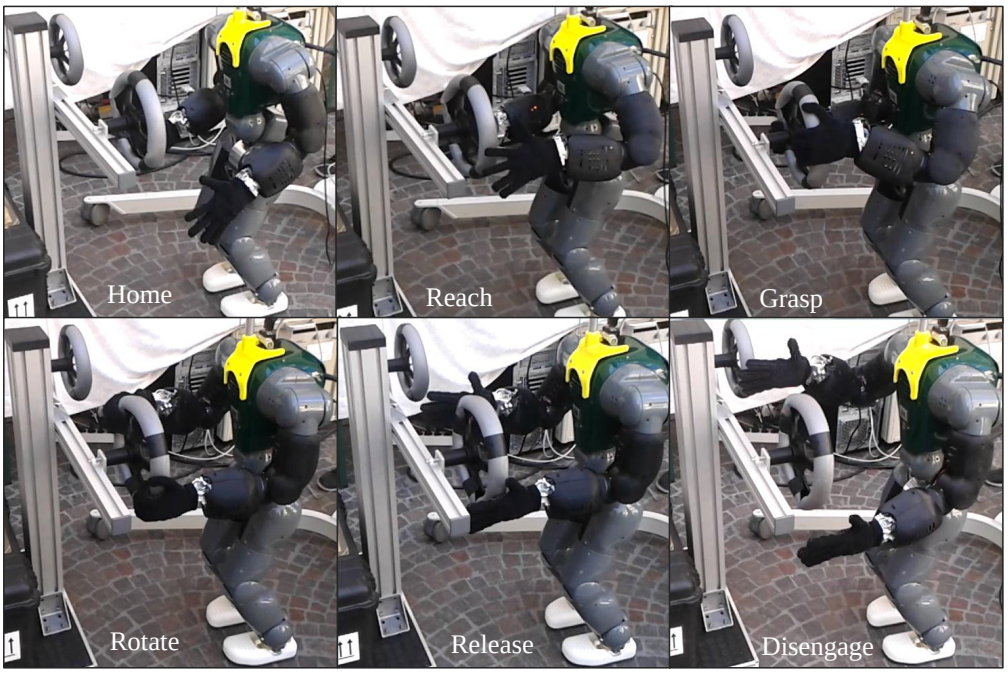

Fig. 6: Valve turning sequences, starting from the home posture: Reach, Grasp, Rotate, Release, Disengage. This sequence is repeated until the valve is open.

tracking of the valve rotation trajectory is realized and e_x is converged to a low value. Acquired interaction forces demonstrate the compliance of the grasp along all directions, except the one coinciding with the valve rotation direction, in which sufficient rotational torques are applied on the valve axis. The realized (red, solid) and the desired (blue, dashed) components of the translational Cartesian stiffness matrix for the right and the left arm endpoints in Rotation primitive are illustrated in Figs. 8 and 9, respectively. Realized stiffness profiles are calculated based on the actual arm configurations, joint stiffness values and external forces [22].

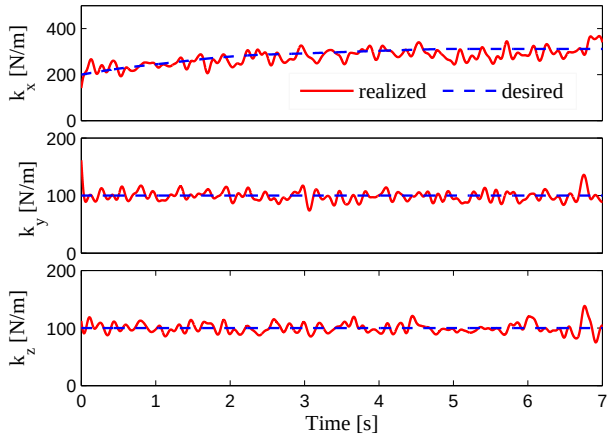

Fig. 8: The desired (blue, dashed) and the realized (red, solid) components of the translational part of the Cartesian stiffness matrix with respect to Σ_R are plotted along x (upper plot), y (middle plot) and z (bottom plot) directions. The valve is rotated along the x direction of Σ_R frame.

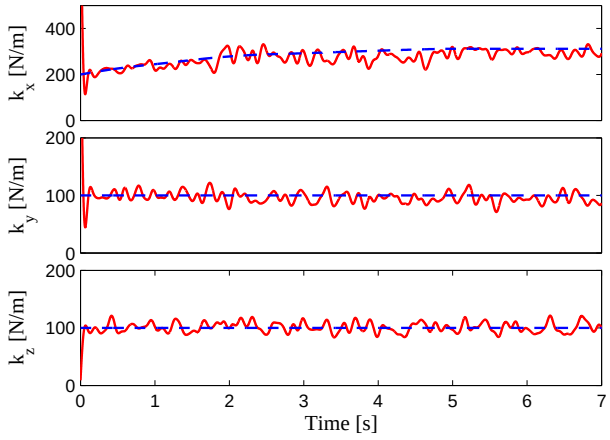

Fig. 9: Left arm stiffness tracking results. The order of the plots is similar to Fig. 8.

To illustrate the efficiency of the proposed update law in generation of the task-required rotational torque (by adjusting the corresponding stiffness component), a similar experiment was performed using a lower friction coefficient on the valve's axis of rotation. As demonstrated in Fig. 10, the stiffness component k_{x_d}, is adjusted and converged to a lower value while the task is being accomplished. This highlights the task-efficiency of the proposed update law in rendering the desired interaction performance.

V. Conclusion

In this work, a control architecture, incorporating a novel manipulation framework for the compliant humanoid robot (COMAN) was proposed and experimentally validated in

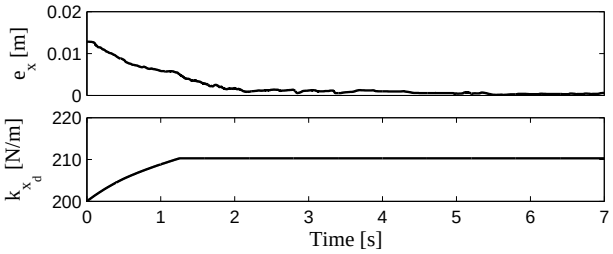

Fig. 10: The maximum tracking error, e_x, and the updated stiffness parameter, k_{x_d}, for an experiment in which the valve friction was adjusted to a lower value compared to Fig. 7.

a valve turning task. The interaction controller established a stable and compliant contact between the SoftHands and the valve to avoid the generation of high interaction forces in contacts. An update law was implemented to adjust the realized Cartesian stiffness profile of the two arm endpoints relying on the existing friction in the valve axis.

Preliminary results of the implementation of COMAN's control framework demonstrated stable and robust manipulation capabilities, highlighting the potential of the underlying techniques for disaster robotics.

ACKNOWLEDGMENT

Authors would like to thank to Corrado Pavan and Valerio Varricchio for their support in setting up the pilot interface. This work is supported in part by the European Research Council under EU FP7-ICT project, WALKMAN, "Whole-body Adaptive Locomotion and Manipulation", no. 611832, and by the European Research Council under the Advanced Grant SoftHands "A Theory of Soft Synergies for a New Generation of Artificial Hands" no. ERC-291166.

REFERENCES

[1] R. R. Murphy, *Disaster robotics*. MIT Press, 2014.

[2] N. G. Tsagarakis, S. Morfey, G. Medrano Cerda, L. Zhibin, and D. G. Caldwell, "Compliant humanoid coman: Optimal joint stiffness tuning for modal frequency control," in *Robotics and Automation (ICRA), 2013 IEEE International Conference on*. IEEE, 2013, pp. 673–678.

[3] C. Borst, T. Wimböck, F. Schmidt, M. Fuchs, B. Brunner, F. Zacharias, P. R. Giordano, R. Konietschke, W. Sepp, S. Fuchs *et al.*, "Rollin'justin-mobile platform with variable base." in *ICRA*, 2009, pp. 1597–1598.

[4] I.-W. Park, J.-Y. Kim, J. Lee, and J.-H. Oh, "Mechanical design of humanoid robot platform khr-3 (kaist humanoid robot 3: Hubo)," in *Humanoid Robots, 2005 5th IEEE-RAS International Conference on*. IEEE, 2005, pp. 321–326.

[5] A. Harris and J. M. Conrad, "Survey of popular robotics simulators, frameworks, and toolkits," in *Southeastcon, 2011 Proceedings of IEEE*. IEEE, 2011, pp. 243–249.

[6] A. A. Medeiros, "A survey of control architectures for autonomous mobile robots," *Journal of the Brazilian Computer Society*, vol. 4, no. 3, 1998.

[7] N. Alunni, C. Phillips-Grafftin, H. B. Suay, D. Lofaro, D. Berenson, S. Chernova, R. W. Lindeman, and P. Oh, "Toward a user-guided manipulation framework for high-dof robots with limited communication," in *Technologies for Practical Robot Applications (TePRA), 2013 IEEE International Conference on*. IEEE, 2013, pp. 1–6.

[8] E. Ackerman, "Darpa robotics challenge trials: What you should (and shouldn't) expect to see," *IEEE Spectrum*, vol. 19, 2013.

[9] M. Orsag, C. Korpela, S. Bogdan, and P. Oh, "Valve turning using a dual-arm aerial manipulator," in *Unmanned Aircraft Systems (ICUAS), 2014 International Conference on*. IEEE, 2014, pp. 836–841.

[10] A. Konno, Y. Hwang, S. Tamada, and M. Uchiyama, "Working postures for humanoid robots to generate large manipulation force," in *Intelligent Robots and Systems, 2005.(IROS 2005). 2005 IEEE/RSJ International Conference on*. IEEE, 2005, pp. 2548–2553.

[11] A. Carrera, S. R. Ahmadzadeh, A. Ajoudani, P. Kormushev, M. Carreras, and D. G. Caldwell, "Towards autonomous robotic valve turning," *Cybernetics and Information Technologies*, vol. 12, no. 3, pp. 17–26, 2012.

[12] A. Ajoudani, N. G. Tsagarakis, and A. Bicchi, "Tele-Impedance: Teleoperation with impedance regulation using a body-machine interface," *International Journal of Robotics Research*, vol. 31(13), pp. 1642–1655, 2012, http://www.youtube.com/watch?v=KPO6IO7Tr-Q.

[13] M. G. Catalano, G. Grioli, A. Serio, E. Farnioli, C. Piazza, and A. Bicchi, "Adaptive synergies for a humanoid robot hand," in *IEEE-RAS International Conference on Humanoid Robots*, 2012.

[14] A. Bicchi, M. Gabiccini, and M. Santello, "Modelling natural and artificial hands with synergies," *Philosophical Transactions of the Royal Society B: Biological Sciences*, vol. 366, no. 1581, pp. 3153–3161, 2011.

[15] G. Metta, P. Fitzpatrick, and L. Natale, "Yarp: Yet another robot platform," *International Journal of Advanced Robotics Systems, special issue on Software Development and Integration in Robotics*, vol. 3, no. 1, 2006.

[16] M. Quigley, K. Conley, B. P. Gerkey, J. Faust, T. Foote, J. Leibs, R. Wheeler, and A. Y. Ng, "Ros: an open-source robot operating system," *ICRA Workshop on Open Source Software*, 2009.

[17] A. Settimi, C. Pavan, V. Varricchio, M. Ferrati, E. Mingo Hoffman, A. Rocchi, K. Melo, N. G. Tsagarakis, and A. Bicchi, "A modular approach for remote operation of humanoid robots in search and rescue scenarios," in *MESAS*, 2014.

[18] Z. Li, N. G. Tsagarakis, and D. G. Caldwell, "A passivity based admittance control for stabilizing the compliant humanoid coman," in *Humanoid Robots (Humanoids), 2012 12th IEEE-RAS International Conference on*. IEEE, 2012, pp. 43–49.

[19] L. Sentis and O. Khatib, "Synthesis of whole-body behaviors through hierarchical control of behavioral primitives," *International Journal of Humanoid Robotics*, vol. 2, no. 04, pp. 505–518, 2005.

[20] S. Chiaverini, "Singularity-robust task-priority redundancy resolution for real-time kinematic control of robot manipulators," *Robotics and Automation, IEEE Transactions on*, vol. 13, no. 3, pp. 398–410, 1997.

[21] T. F. Chan and R. V. Dubey, "A weighted least-norm solution based scheme for avoiding joint limits for redundant joint manipulators," *Robotics and Automation, IEEE transactions on*, vol. 11, no. 2, pp. 286–292, 1995.

[22] S.-F. Chen and I. Kao, "Conservative congruence transformation for joint and cartesian stiffness matrices of robotic hands and fingers," *The International Journal of Robotics Research*, vol. 19, no. 9, pp. 835–847, 2000.

[23] A. Ajoudani, M. Gabiccini, N. G. Tsagarakis, A. Albu-Schäffer, and A. Bicchi, "TeleImpedance: Exploring the role of common-mode and configuration-dependant stiffness," in *IEEE International Conference on Humanoid Robots*, 2012.

[24] A. Albu-Schaffer and G. Hirzinger, "Cartesian impedance control techniques for torque controlled light-weight robots," in *Robotics and Automation, 2002. Proceedings. ICRA'02. IEEE International Conference on*, vol. 1. IEEE, 2002, pp. 657–663.

[25] M. Mosadeghzad, G. A. Medrano-Cerda, J. A. Saglia, N. G. Tsagarakis, and D. G. Caldwell, "Comparison of various active impedance control approaches, modeling, implementation, passivity, stability and trade-offs," in *Advanced Intelligent Mechatronics (AIM), 2012 IEEE/ASME International Conference on*. IEEE, 2012, pp. 342–348.

[26] A. Albu-Schäffer, C. Ott, and G. Hirzinger, "A unified passivity-based control framework for position, torque and impedance control of flexible joint robots," *The International Journal of Robotics Research*, vol. 26, no. 1, pp. 23–39, 2007.

[27] C. Ott, *Cartesian impedance control of redundant and flexible-joint robots*. Springer, 2008, vol. 49.

[28] E. Mingo, E. Traversaro, A. Rocchi, M. Ferrati, A. Settimi, A. Romano, A. Natale, A. Bicchi, G. Greco, M. Guiggiani, G. Tonietti, F. Nori, and N. Tsagarakis, "Yarp based plugins for gazebo simulator," in *2014 Modelling and Simulation for Autonomous Systems Workshop (MESAS)*, Roma, Italy, 5 -6 May 2014, 2014.